




Deformation Behavior, Structure and Properties of an Equiatomic Ti–Ni Shape Memory Alloy Compressed in a Wide Temperature Range

Victor Komarov^{1,2,3}  · Irina Khmelevskaya¹ · Roman Karelin^{1,2} · Ivan Postnikov¹ · Grzegorz Korpala³ · Rudolf Kawalla³ · Ulrich Prahl³ · Vladimir Yusupov² · Sergey Prokoshkin¹

Received: 10 March 2021 / Accepted: 2 July 2021 / Published online: 24 July 2021
© The Indian Institute of Metals - IIM 2021

Abstract In the present work, flow curves of an equiatomic Ti–Ni shape memory alloy after deformation by compression in the temperature range from 100 to 900 °C at a strain rate of 1 s^{-1} and up to a true strain (ϵ) of 0.9 were obtained. The phase composition, mechanical and functional properties after compression to $\epsilon = 0.5$ were studied. The boundaries of the temperature ranges of the development of dynamic softening processes were determined, as follows: dynamic recovery in 100–300 °C range; dynamic polygonization in 300–500 °C range and dynamic recrystallization above 500 °C. An optimum deformation temperature range in terms of accumulation of high strains and achieving improved functional properties is 300–500 °C. It has also been found that post-deformation annealing at temperatures above the deformation temperature leads to the decrease in the B2-austenite lattice defectness and to a significant increase in shape recovery characteristics.

Keywords Shape memory alloys · Compression · Deformation behavior · Ti–Ni · Thermomechanical treatment · Functional properties

1 Introduction

Shape memory alloys (SMA) are among the most promising and actively developed functional materials of the present time [1–6]. These materials have the unique properties of recovering their original shape after deformation when the load is removed (superelasticity effect, SE) or when heated (shape memory effect, SME). Ti–Ni-based SMA are widely used in different fields of engineering for production of various shape memory devices [1, 5, 7, 8]. Modern materials science is moving in the direction of developing production technologies to maximally implement the potential of functional properties innated to the applied alloys.

Functional and mechanical properties of Ti–Ni SMA are structure-sensitive and can be greatly improved by the formation of well-developed dislocation substructure or ultrafine-grained structure using various modes of thermomechanical treatment (TMT), including severe plastic deformation (SPD) [9–15]. It was shown in [16, 17] that the formation of an ultrafine-grained structure allows to increase the maximum completely recoverable strain up to 9%.

Conventional technologies of Ti–Ni SMA manufacturing include various deformation treatments at temperatures above 700 °C [18–22]. These processing modes allow obtaining rods and sheets only with a recrystallized structure, which is characterized by decreased properties. The development of manufacturing technologies is constrained by the lack of systematic data on structure formation and deformation behavior in a wide temperature range of an equiatomic Ti–Ni SMA.

Application of various deformation regimes for obtaining predetermined structural state in Ti–Ni SMA, which is used for medical or technical purposes, requires a deeper

✉ Victor Komarov
vickomarov@gmail.com

¹ National University of Science and Technology MISIS, Leninskiy pr. 4, Moscow, Russia

² Baikov Institute of Metallurgy and Materials Science RAS, Leninskiy pr. 49, Moscow, Russia

³ TU Bergakademie Freiberg, Bernhard-von-Cotta Str. 4, Freiberg, Germany

knowledge of features of the structure formation during the development of dynamic softening and hardening processes. The fundamental approach of the investigation of the deformation behavior for the determination of optimal deformation modes by the construction of the flow curves after compression in the temperature range from 600 to 1000 °C was applied in the study [19] for an equiatomic Ti–Ni and Ti–Ni–Fe alloys.

Features of the structure formation in the bulk Ti–Ni SMA samples in the temperature range below 600 °C are basically studied after severe plastic deformation (SPD) under high strains (cold rolling, high pressure torsion, ECAP) [15, 16, 23–26]. Therefore, to systemize the previously obtained knowledge on the deformation behavior of Ti–Ni SMA at temperatures below 600 °C, additional studies with application of the more common deformation modes are required.

Detailed analyses of the flow curves, obtained after compression of the hyper-equiatomic nickel-rich Ti–50.9at%Ni alloy in the temperature range from 100 to 1000 °C, allowed determining temperature ranges for the development of dynamic softening processes, as follows: dynamic recovery from 100 to 300 °C, dynamic polygonization from 300 to 600 °C and dynamic recrystallization above 600 °C [27]. It was shown, that the dynamic polygonization process, which consists in the formation of polygonal subgrains during deformation, leads to a significant improvement of mechanical properties and also allows accumulation of high strains because of reaching a steady-state stage of deformation. However, in this alloy, deformation in the temperature range of 250–500 °C is accompanied by the dynamic strain aging with precipitation of Ni_4Ti_3 particles, which have a great impact on phase transformations, properties and structure formation. This feature of aging Ti–Ni alloys leads to significant differences as compared to an unaged equiatomic Ti–Ni SMA [1, 11, 14]. These conditions make a similar study of the equiatomic alloy topical.

Thus, the goal of this work is to determine the temperature ranges for the development of dynamic softening processes (recovery, polygonization and recrystallization) in an equiatomic Ti–Ni SMA. The deformation behavior, structure and properties development are studied after compression in the temperature range of 100–900 °C. The effect of post-deformation annealing (PDA) on Ti–Ni SMA properties is studied as well.

2 Materials and experimental methods

The material used in the present study was an equiatomic Ti–50.0at%Ni alloy, supplied by The industrial center MATEK-SMA Ltd (Table 1). A 5-mm-diameter rod

obtained by hot forging and annealed at 700 °C for 30 min, followed by water quenching served as the reference treatment (RT). Then RT cylindrical specimens with a diameter of 5 mm and a height of 10 mm were cut from rods for performing compression tests.

Compression tests were performed on the hot-forming simulator “WUMSI”, which was also used to obtain flow curves and determine material characteristics. Tests were made at a deformation rate of 1 s^{-1} with the true (logarithmic) strain (e) of 0.5 for the study of structure and properties and $e = 0.9$ for the study of deformation behavior in a temperature range from 100 to 900 °C. A graphite-based lubricant was applied to the specimen for reducing the friction and minimizing the tensile stresses. Post-deformation annealing (PDA) at a temperature of 400 °C for 1 h in an air furnace followed by water cooling was applied to analyse the stability of the structure and properties after TMT.

The phase composition after deformation by compression was examined by X-ray diffraction using a “DRON-3.0” ($U = 30 \text{ kV}$, $I = 25 \text{ mA}$, $\text{CuK}\alpha$ radiation) diffractometer. The width of diffraction peak corresponding to (020) $\text{B19}'$ -martensite line was examined to evaluate the extent of deformation hardening. To evaluate the change in mechanical properties after compressive deformation at different temperatures, the Vickers hardness (HV_1) at 7 points in different regions of the specimens was measured. The measurements were performed at room temperature using the hardness tester “Metolab 421” under a load of 9.8 N (1 kg) for a dwell time of 10 s.

The shape recovery characteristics were determined via a thermomechanical method that includes bending at room temperature followed by heating above A_f . Temperature range of shape recovery (TRSR) was measured as the difference between finishing and starting (A_s) temperatures of reverse martensitic transformation ($A_f - A_s$). Samples of $0.3 \times 0.4 \times 8 \text{ mm}$ dimensions were bent over cylindrical mandrels with various diameters to vary the total induced strain (ϵ_i) from 1.3 to 13%. The induced strain (ϵ_i) after superelastic unloading (due to superelasticity effect, ϵ_r^{SE}), residual strain (ϵ_r) after heating and the corresponding recovery strain (due to shape memory effect, ϵ_r^{SME}) were determined using the arc templates (Fig. 1). The shape recovery rate (SRR) was measured as a ratio of the recovery strain to induced strain. The value of the maximum completely recoverable strain ($\epsilon_{rt,1}$) corresponds to the highest value (ϵ_{rt}) attained at $\text{SSR} = 100\%$.

Table 1 Chemical composition of the alloy studied (wt%)

Ni	Ti	C	O	N	H	Other
54.95*	Balance	< 0.040	< 0.042	< 0.003	< 0.002	< 0.1

*Equal to 50.0at%Ni

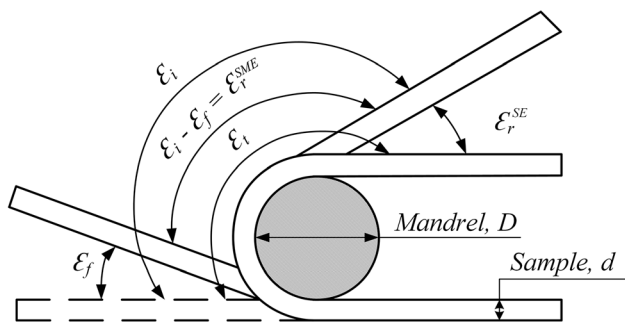


Fig. 1 Various components of shape recovery characteristics

3 Results and Discussion

3.1 Deformation Behavior

Flow curves of an equiatomic Ti–Ni SMA, obtained by compression in the temperature range from 100 to 900 °C at a strain rate of 1 s⁻¹ up to $e = 0.9$, are shown in Fig. 1. Compression is not accompanied by the formation of cracks in the whole temperature range from 900 to 100 °C (Fig. 2). In this temperature range, the phase composition of the alloy is an austenitic B2-phase. The shapes of flow curves correspond to the general patterns of hot, warm and cold deformation. It is determined by the predominance and competition of two processes, developed during deformation—dynamic hardening or dynamic softening. With increasing deformation temperature, the dynamic

softening gains even more significantly during deformation.

At the deformation temperatures of 600–900 °C, the steady-state stage is quickly reached at the strain (e) of < 0.1. The lowering of the deformation temperature leads to the shift of the steady-state stage toward higher true strain values (e_{ss}). The steady-state stress (σ_{ss}) increases from 120 to 380 MPa with decreasing deformation temperature from 900 to 600 °C. Further decrease in deformation temperature from 600 to 500 °C leads to a significant increase of the steady-state strain (e_{ss}) from 0.07 to 0.21 and steady-state stress (σ_{ss}) from 380 to 530 MPa. Thus, it can be assumed, that the temperature of 500 °C is the upper limit of dynamic polygonization processes. Deformation at 400 °C leads to the formation of the steady-state stage, while after deformation at 300 °C, the steady-state stage is no longer observed. The temperature of 300–400 °C could therefore be considered as a lower limit for the dynamic polygonization process (Fig. 2). In the temperature range of 400–900 °C, the dynamic hardening and dynamic softening processes are balanced. Therefore, this temperature range can be used to accumulate higher strains.

The decrease in the deformation temperature from 300 to 100 °C leads to the change of the slope of the flow curves. This indicates the increase of deformation hardening. At the temperature of 100 °C, the value of deformation hardening is maximum, and the flow stress at $e = 0.9$ exceeds 1800 MPa. The graphical representation of the influence of the deformation temperatures on the maximum deformation stress, σ_{max} (or stress at $e = 0.9$), and the corresponding maximum deformation strain (e_{max}), as well as the steady-state stress (σ_{ss}) and the steady-state strain (e_{ss}) are presented in Fig. 3.

The maximum deformation stress, σ_{max} (or the stress at the true strain of $e = 0.9$, where the steady-state stage is not achieved), decreases rapidly with an increase in the deformation temperature. The largest decrease of σ_{max} occurs in the temperature range of 100–300 °C. Further, this process is inhibited by the increase in deformation temperature. This temperature dependence is typical for the development of recovery processes in the equiatomic Ti–Ni SMA, since there is no precipitation of the Ti₃Ni₄ phase [1, 27]. The flow curves become smoother after deformation at the temperature of 600 °C and higher. The e_{max}

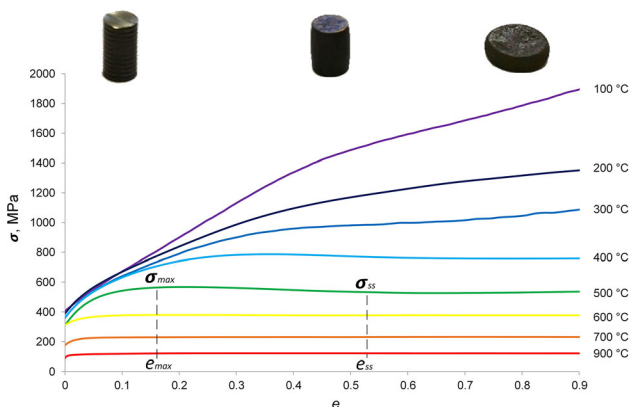


Fig. 2 Flow curves for Ti–50.0at%Ni alloy obtained in a temperature range from 100 to 900 °C at a strain rate of 1 s⁻¹

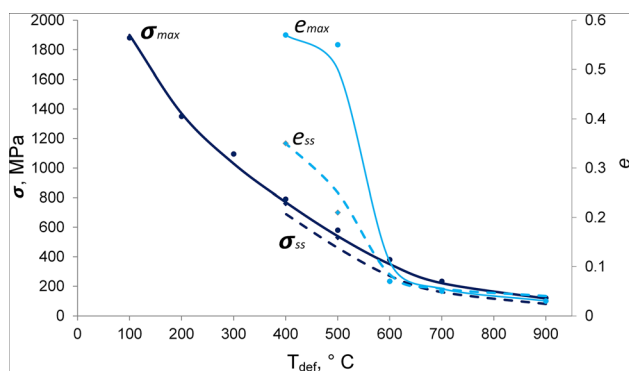


Fig. 3 Values of maximum deformation stress (σ_{\max} at $e = 0.9$), steady-state stress (σ_{ss}), maximum deformation strain (e_{\max}) and the steady-state strain (e_{ss}) depending on the deformation temperature

values are stabilized at the deformation temperature of 600 °C and do not exceed 0.1. This trend confirms the assumption that the temperature range of 300–500 °C is the range for the dynamic polygonization processes.

Thus, the compression at temperatures of 400–900 °C at a strain rate of 1 s^{-1} is accompanied by the appearance of a steady-state stage and accumulating high strain degrees. The polygonised substructure can be achieved in a wide temperature range of 300–500 °C at strains of $e > 0.5$.

3.2 Phase and structural analysis

A study of the structural state of the equiatomic Ti–Ni alloy at room temperature after compression at lower deformation temperatures by the TEM does not seem to be informative. In an earlier study, the structure of Ti–50.0at%Ni alloy was studied using TEM after compression in the temperature range of 500–900 °C followed by water cooling [19].

After compression at 500 °C, the structure of B2-austenite is partially recrystallized (Fig. 4 a). The B19'-martensite crystals are found inside small (2–3 μm diam.) recrystallized grains, while in non-recrystallized areas, they inherit subgrains of the austenite polygonised dislocation

substructure. Thus, under compressive deformation, the dynamic recrystallization begins at 500 °C. After compression at 600 °C, the austenite is almost completely recrystallized (Fig. 4b). The structure after deformation at 700–900 °C shows coarser recrystallized grains with twinned martensite crystals inside (Fig. 4c). After deformation in the lower temperature range (100–400 °C), the dislocation substructure of deformed B2-austenite is inherited by the growth (during cooling) of B19'-martensite crystals. The dislocation substructure of B2-austenite overlaps with the B19'-martensite structure. Thus, the structural analysis allows to establish only the upper boundary of dynamic polygonization temperature region (500 °C).

Based on the foregoing discussions in the present study, the deformation hardening of the alloy after compression is estimated by the change in the width of the XRD diffraction peak corresponding to the plane (002) of B19'-martensite and by the change in the hardness value.

X-ray structural analysis at room temperature shows that after RT, predominantly a monoclinic B19'-martensite phase is present. After deformation in the austenitic state in the temperature range of 200–700 °C, the phase composition after cooling to room temperature does not change qualitatively and is called B19'-martensite (thermally and plastically deformed), and the weak peaks (just above the background) correspond to the B2- or R- phases, (Fig. 5 a, deformation at 500–700 °C). After deformation at 100 °C, along with the peaks corresponding to B19'-martensite, prominent peaks of B2-austenite ($2\theta = 42.5^\circ$) and R-phase appear (Fig. 5 a, deformation at 100 °C). Stress fields from the austenite substructure formed at low deformation temperatures as compared to higher temperatures of 500–700 °C stimulate a more complete B2 \rightarrow R transformation upon cooling to room temperature. The peak corresponding to the B2-phase indicates plastically deformed austenite. The variations of the width of the XRD peak corresponding to (002) B19' are given by Fig. 5 b. Examination of this characteristic after compression and

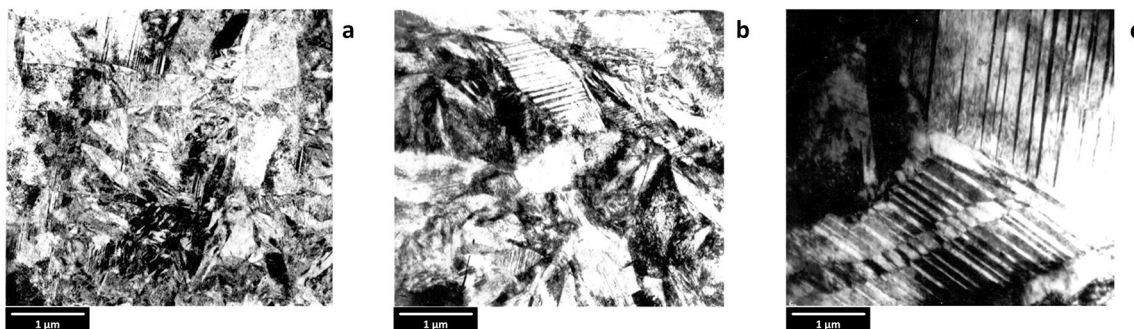


Fig. 4 Structure of Ti–50.0 at%Ni alloy after compression at 500 °C (a), 600 °C (b) and 900 °C (c) as revealed by the transmission electron microscopy (bright field) images. Adapted from [28]

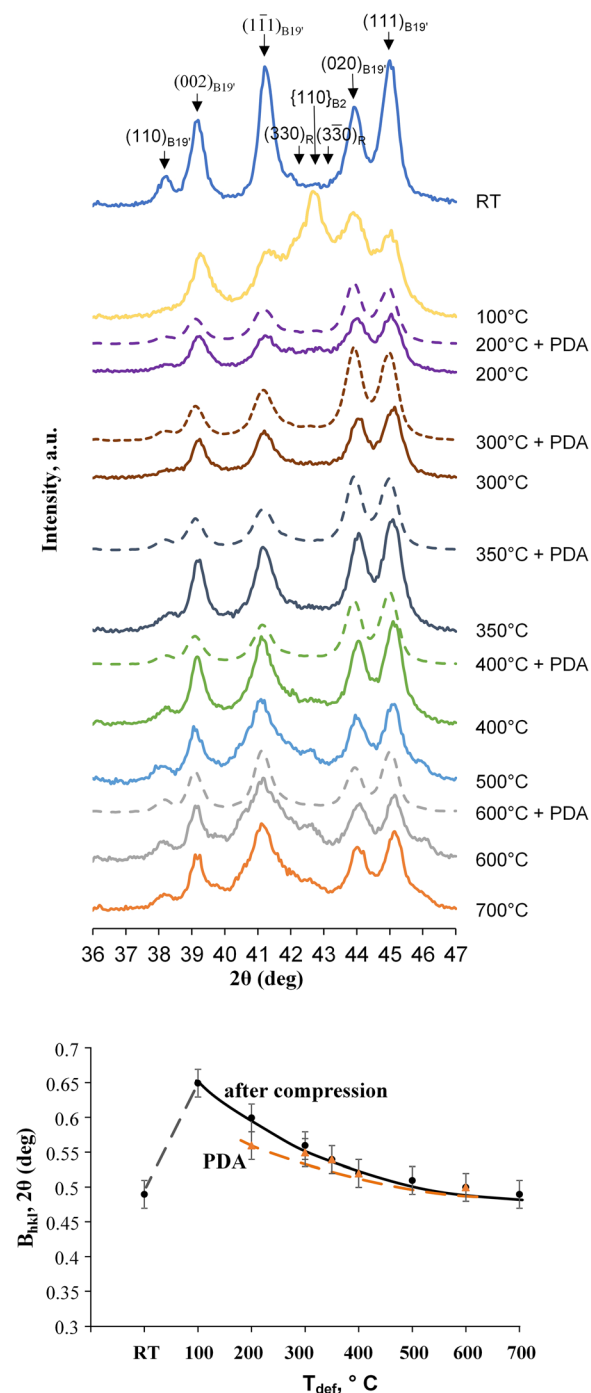


Fig. 5 X-ray diffractograms of Ti–50.0at.%Ni alloy at RT, after compression at 100–700 °C and PDA (a), and the dependence of B(002)_{B19'} XRD peak width on the deformation temperature (b)

RT shows that the peak narrows down from 0.65° to 0.5° with an increase in the deformation temperature from 100 to 700 °C. This indicates a decrease in the extent of crystal lattice defects. The most noticeable change ($\Delta 2\theta = 0.15$) is observed in the deformation temperature range of 100–500 °C in comparison with the range of 500–700 °C, where $\Delta 2\theta = 0.03$. These results indicate temperature

a

ranges for the development of the processes of dynamic recovery and dynamic polygonization (100–500 °C) and dynamic recrystallization (500–700 °C).

3.3 Mechanical and functional properties

Deformation hardening of Ti–50.0at.%Ni SMA after compression was also estimated by the change in the hardness values which also indicate the temperature ranges of softening processes. The graphical representation of average HV₁ hardness values for samples after deformation at various temperatures and after RT are shown in Fig. 6. A decrease in the deformation hardening with an increase in the deformation temperature indicates a decrease in structural defects and dislocation density. The nature of the hardness curve is comparable to the decrease in the peak width, (002) B19'-martensite (Fig. 5b). The rate of decrease in hardness is most rapid in the range of 100–500 °C, and slows down above 500 °C. Thus, based on the results of hardness tests and the change in the width of XRD peak, the starting temperature of the recrystallization process can be defined. However, the temperature ranges of recovery and polygonization processes cannot be precisely split, as it was suggested based on analyses of flow curves.

The maximum hardness value (HV₁) of 300 HV is observed after deformation at 100 °C. Relatively lower hardness values (230–250 HV) remain after deformation at 200–500 °C. At a deformation temperature of 700 °C and higher, the hardness value approaches that of the reference treatment, which indicates the development of dynamic recrystallization process. The temperature range for obtaining high mechanical characteristics is 100–500 °C.

Annealing of Ti–50.0at.%Ni SMA at 400 °C, for 1 h after compression at different temperatures does not lead to a change in hardness values as compared to the deformed

b

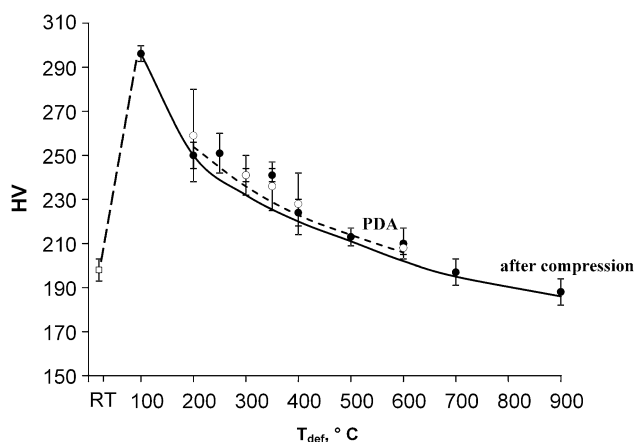


Fig. 6 Dependence of the Vickers hardness value (HV₁) on the deformation temperature

state (Fig. 6). At a temperature of 400 °C, the alloy still retains the developed dislocation substructure of B2-austenite showing high dislocation density, which, apparently, does not allow the development of strong softening process during PDA after low-temperature deformation. After deformation above 400 °C, additional annealing below deformation temperature does not cause significant structural changes.

The strength characteristics of Ti–Ni SMA, such as the yield stress, which can be estimated by the hardness value, strongly determine the value of recoverable strain [1]. The growth of deformation hardening indicates the growth of the true yield stress. At the same time, “transformation” yield stress does not change because almost constant phase composition (B19'-martensite) at room temperature after deformation in the investigated temperature range is observed (except compression at 100 °C, that results in a significant increase of the R-phase amount, Fig. 5a). Thus, the difference between true and «transformation» yield stresses increases, and the process of dislocation slips is later involved in the general deformation process and, consequently, the value of recoverable strain is expected to increase [1].

From thermomechanical bending tests, it is shown that after compression in the temperature range of 100–350 °C, the SE recovery strain (ε_r^{SE}) is greater than the SME recovery strain (ε_r^{SME}) in the whole range of induced strains from 1.3 to 13%. Deformation in the temperature range of 400–900 °C changes this ratio in favor of ε_r^{SME} . PDA at 400 °C for 1 h at the temperature below deformation temperature provides the increase in the ratio of ε_r^{SE} to ε_r^{SME} . PDA at equal to or above the deformation temperature does not change the ratio of ε_r^{SE} to ε_r^{SME} .

The highest values of total recoverable strain, $\varepsilon_{rt} = 11\%$, including shape recovery due to SE and SME, are obtained after deformation at 350–500 °C. The shape recovery rate (SRR) of 80% and more after induced strain ($\varepsilon_i = 8\%$) is observed in the temperature range of 400–500 °C, also corresponding to dynamic polygonization process (Fig. 7 a). PDA at 400 °C after compression at low temperatures (up to 300 °C) increases the SRR from 75–77% to 87–90%. At the same time, the PDA after compression at 400 °C and higher does not change the SRR.

The values of completely recoverable strain ($\varepsilon_{rt,1}$) is about 3% in all deformation regimes studied (Fig. 7 b). PDA at the temperature of 400 °C for 1 h leads to the increase of $\varepsilon_{rt,1}$ from 2.5–3 to 4.5–5% for the samples obtained by compression in the temperature range of 100–500 °C. PDA of samples, compressed at the other temperatures, do not change the value of $\varepsilon_{rt,1}$, which can be explained by the formation of a stable recrystallized structure after deformation.

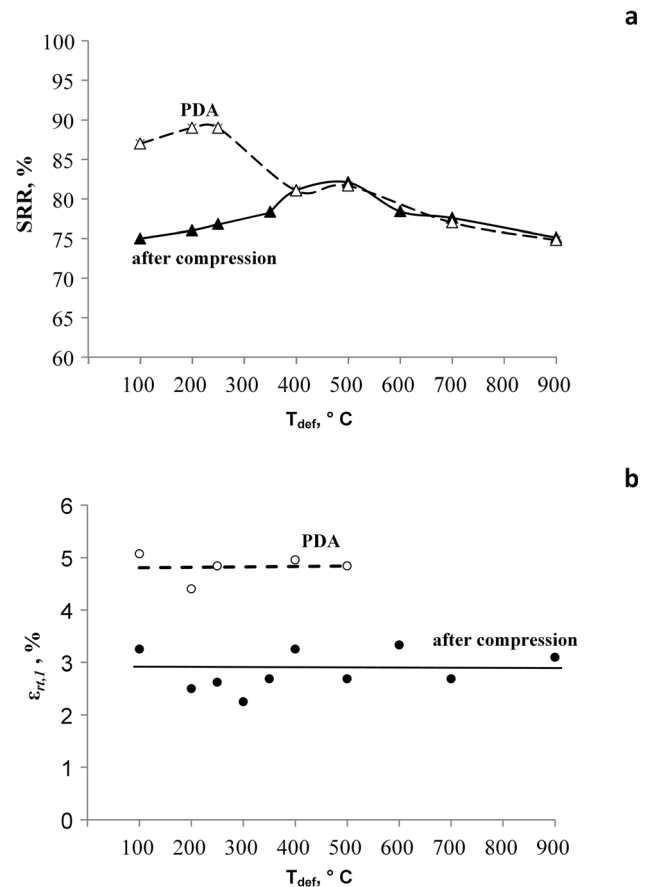


Fig. 7 Effect of deformation temperature on **a** shape recovery rate and **b** total completely recoverable strain before and after PDA

In an equiatomic Ti–Ni SMA, after RT, the temperature of the reverse martensitic transformation, A_s – A_f = 66–86 °C, the change in temperature range of shape recovery (TRSR) depending on the deformation temperature, is determined by the extent of lattice defects after deformation, and the value of the induced strain [1]. After deformation at 100 and 200 °C, TRSR decreases by 10 °C (Fig. 8). The decrease in the magnitude of deformation hardening due to the development of the processes of recovery, polygonization and recrystallization leads to a shift in the TRSR to the region of higher temperatures. The

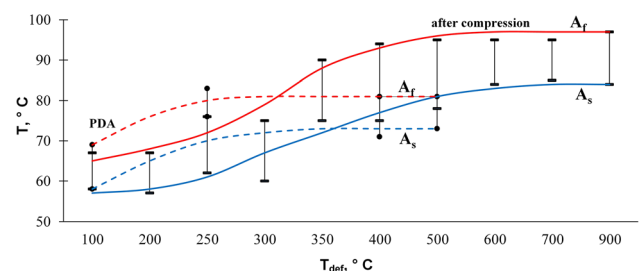


Fig. 8 Effect of deformation temperature and PDA on the temperature range of shape recovery A_s – A_f (total induced strain, $\varepsilon_i \approx 3\%$)

increase in the induced strain degree from 3 to 8% leads to a shift in the TRSR toward higher temperatures by 10–20 °C. These results define the limits of possibilities for adjustment of the TRSR by the change of the value of the induced strain. Starting from a deformation temperature of 350 °C with an induced deformation of 3% and 8%, the TRSR stabilizes at a temperature of 80–100 °C. PDA increases the position of TRSR in the case of compression in the temperature range of 250–500 °C (Fig. 8).

PDA affects the contribution of ϵ_r^{SE} to ϵ_r^{SME} ratios in cases where the TRSR increases. An increase in TRSR and, consequently, an increase in the M_s temperature with respect to the deformation temperature, promotes a set of deformation due to the reorientation of B19'-martensite and shape recovery due to SME.

Thus, a general pattern of the formation of the functional properties of equiatomic Ti–Ni SMA is revealed. If the PDA temperature is higher than the deformation temperature, then there are changes in the structure of the deformed alloy due to the development of the processes of recovery and polygonization, and the shape recovery is significantly increased; if the PDA temperature is lower than the deformation temperature, then PDA does not significantly affect the structure and functional properties.

Thus, a comparative study of the flow curves, hardness, width of XRD peaks and functional properties of Ti–50.0at%Ni alloy was done. Deformation in a wide temperature range (100–900 °C) allows to determine the boundaries of the temperature ranges of dynamic softening processes during compression at a strain rate of 1 s^{-1} . The temperature range of dynamic recovery of the alloy is 100–300 °C, which follows from the low kinetics of softening processes and a large amount of structural defects. The dynamic polygonization area is 300–500 °C, as evidenced by the accelerated decrease in the XRD peak width. The temperature range of dynamic recrystallization is 500–700 °C, which is confirmed by structural analysis, as well as by a rapid decrease in stress on the flow curves, stabilization of the XRD peak width of B19'-martensite and hardness.

4 Conclusions

1. The deformation temperature of 300 °C is a boundary between the high-temperature and low-temperature types of deformation behavior for the equiatomic Ti–Ni SMA. It marks the transition from the flow curves of “high temperature” type (with a steady-state stage) to the “low temperature” type (without a steady-state stage).
2. The temperature ranges for the development of dynamic softening processes in the equiatomic Ti–Ni

shape memory alloy after deformation by compression at $T = 100\text{--}900 \text{ °C}$ and $\dot{\epsilon}$ of 1 s^{-1} are determined, as follows: dynamic recovery in 100–300 °C range; dynamic polygonization in 300–500 °C range and dynamic recrystallization above 500 °C.

3. The optimum deformation temperature range for Ti–50.0at%Ni alloy in terms of accumulation of high strains due to the onset of a steady-state stage of deformation and improving the functional properties is the temperature range of dynamically polygonized substructure formation (300–500 °C).
4. Post-deformation annealing at temperatures above the deformation temperature leads to a decrease in the B2-austenite lattice defects and, consequently, increases shape recovery characteristics. PDA at the temperature equal to the deformation temperature or below does not lead to significant changes in the lattice defects.

Acknowledgements The reported study was funded by RFBR (project number 19-33-60090) in the part of thermomechanical treatment and study of deformation behavior; by the Ministry of Science and Higher Education of the Russian Federation in the framework of the State Task (project code 0718-2020-0030) in the part of structural and X-ray analysis and study of properties. V. Komarov is grateful to “Mikhail Lomonosov” joint program of DAAD and Ministry of Science and Higher Education of the Russian Federation for the opportunity to conduct research in Germany.

References

- [1] Brailovski V, Prokoshkin S, Terriault P, Trochu P, *Shape Memory Alloys: Fundamentals, Modeling and Applications*, ETS, Montreal (2003) p 844. <https://espace2.etsmtl.ca/id/eprint/3754>
- [2] Lagoudas D C, *Shape memory alloys: modeling and engineering applications*, (ed) Dimitris C, Springer Science and Business Media (2008) p 436. <https://doi.org/10.1007/978-0-387-47685-8>
- [3] Raju T N, and Sampath V, *Trans Ind Inst Met* **64**(1-2) (2011) 165. <https://doi.org/https://doi.org/10.1007/s12666-011-0032-6>
- [4] Duerig T W, Melton K N, Stöckel D W C M, *Engineering aspects of shape memory alloys*, Butterworth-Heinemann (2013) p 451.
- [5] Jani J M, Leary M, Subic A, Gibson M A, *Mater Des* **56** (2014) 1078. <https://doi.org/https://doi.org/10.1016/j.matdes.2013.11.084>
- [6] Santosh S, and Sampath V, *Trans Ind Inst Met* **72** (6) (2019) 1481. <https://doi.org/https://doi.org/10.1007/s12666-019-01604-4>
- [7] Manam N S, Harun W S W, Shri D N A, Ghani S A C, Kurniawan T, Ismail M H, Ibrahim M H I, *J Alloys Compd* **701** (2017) 698. <https://doi.org/https://doi.org/10.1016/j.jallcom.2017.01.196>
- [8] Rykлина E, Korotitskiy A, Khmelevskaya I, Prokoshkin S, Polyakova K, Kolobova A, Chernov A, *Mater Des* **136** (2017)174. <https://doi.org/https://doi.org/10.1016/j.matdes.2017.09.024>
- [9] Valiev R, Gunderov D, Prokofiev E, Pushin V, and Zhu Y, *Mater Trans* **49** (2008) 97. <https://doi.org/https://doi.org/10.2320/matertrans.ME200722>

- [10] Khmelevskaya I Y, Kawalla R, Prokoshkin S D, Komarov V S, *IOP Conf Ser: Mater Sci Eng* **63** (2014) 012108. <https://doi.org/https://doi.org/10.1088/1757-899X/63/1/012108>
- [11] Polyakova-Vachiyana K A, Ryklina E P, Prokoshkin S D, and Dubinskii S M, *Phys Met Metallogr* **117** (8) (2016) 817-827. <https://doi.org/https://doi.org/10.1134/S0031918X16080123>
- [12] Gunderov D, Churakova A, Lukyanov A, Prokofiev E, Pushin V, Kreitberg A, and Prokoshkin S, *Mater Today: Proc* **4** (2017) 4825-4829. <https://doi.org/https://doi.org/10.1016/j.matpr.2017.04.078>
- [13] Khmelevskaya I, Komarov V, Kawalla R, Prokoshkin S, and Korpala G, *Mater Today: Proc* **4** (2017). 4830-4835. <https://doi.org/https://doi.org/10.1016/j.matpr.2017.04.079>
- [14] Polyakova K, Ryklina E, and Prokoshkin S, *Mater Today: Proc* **4** (2017) 4836-4840. <https://doi.org/https://doi.org/10.1016/j.matpr.2017.04.080>
- [15] Khmelevskaya I Y, Karelin R D, Prokoshkin S D, Isaenkova M G, Perlovich Y A, Fesenko V A, Zaripova M M, *IOP Conf. Ser.: Mater Sci Eng* **503** (2019) 012024. <https://doi.org/10.1088/1757-899X/503/1/012024>
- [16] Komarov V, Khmelevskaya I, Karelin R, Prokoshkin S, Zaripova M, Isaenkova M, Kawalla R, *J Alloys Compd* **797** (2019) 842. <https://doi.org/10.1016/j.jallcom.2019.05.127>
- [17] Brailovski V, Prokoshkin S, Khmelevskaya I, Inaekyan K, Demers V, Dobatkin S, and Tatyana E, *Mater Trans* **47** (3), (2006), pp. 795-804. <https://doi.org/10.2320/matertrans.47.795>
- [18] Fernandes F M B, Shape Memory Alloys Processing, Characterization and Applications, InTech, Croatia (2013) p 278. <https://doi.org/10.5772/257>
- [19] Prokoshkin S D, Kaputkina L M, and Bondareva S A, *Phys. Met. Metallogr.* **70** (3) (1991) 144.
- [20] Sheremetyev V A, Akhmadkulov O, Komarov V S, Korotitsky A V, Galkin S P, Andreev V A, and Prokoshkin S D, *IOP Conf Ser: Mater Sci Eng* **1008** (2020) 012042. <https://doi.org/https://doi.org/10.1088/1757-899X/1008/1/012042>
- [21] Adarsh S H, and Sampath V, *Intermetallics* **115** (2019) 106632. <https://doi.org/https://doi.org/10.1016/j.intermet.2019.106632>
- [22] Xuan T D, Sheremetyev V A, Komarov V S, Kudryashova A A, Galkin S P, Andreev V A, Brailovski V, *Russ J Non-ferrous Metals* **62** (2021) 39. <https://doi.org/https://doi.org/10.3103/S1067821221010168>
- [23] Prokoshkin S, Khmelevskaya I, Andreev V, Karelin R, Komarov V, Kazakbiev A, *Mater Sci Forum* **918** (2018) 71. <https://doi.org/https://doi.org/10.4028/www.scientific.net/MSF.918.71>
- [24] Khmelevskaya I, Komarov V, Kawalla R, Prokoshkin S, Korpala G, *J Mater Eng Perform* **28** (8) (2017) 4011. <https://doi.org/https://doi.org/10.1007/s11665-017-2841-1>
- [25] Komarov V, Khmelevskaya I, Karelin R, Yusupov V, Kawalla R, Korpala G, Prokoshkin S, *IOP Conf Ser: Mater Sci Eng* **1014** (2021) 012019. <https://iopscience.iop.org/article/https://doi.org/10.1088/1757-899X/1014/1/012019>
- [26] Karelin R D, Khmelevskaya I Y, Komarov V S, Andreev V A, Perkas M M, Yusupov V S, Prokoshkin S D, *J. Mater. Eng. Perform.*, **30** (4) (2021) 3096. <https://doi.org/https://doi.org/10.1007/s11665-021-05625-3>
- [27] Komarov V, Khmelevskaya I, Karelin R, Kawalla R, Korpala G, Prah U, Yusupov V, Prokoshkin S, *JOM* **73**(2) (2021) 620. <https://doi.org/https://doi.org/10.1007/s11837-020-04508-7>
- [28] Bondareva S A, Creation of a substructure during thermomechanical treatment to control transformation parameters and properties of shape memory alloys, Ph D Thesis, MISIS, Russia (1992).

Publisher's Note Springer Nature remains neutral with regard to jurisdictional claims in published maps and institutional affiliations.